

## Structural features of Ni-Cr-Si-B materials obtained by different technologies

E E Kornienko<sup>1</sup>, A A Nikulina<sup>1</sup>, N S Belousova<sup>1</sup>, D V Lazurenko<sup>1</sup>, A S Ivashutenko<sup>2</sup> and V I Kuz'min<sup>3,4</sup>

<sup>1</sup> Faculty of Mechanical Engineering and Technologies, Novosibirsk State Technical University, 20 Prospekt K. Marksa, Novosibirsk, 630073, Russia

<sup>2</sup> Department of Industrial Electric Power Supply, Institute of Power Engineering, Tomsk Polytechnic University, 30 Lenin Avenue, Tomsk, 634050, Russia

<sup>3</sup> Khristianovich Institute of Theoretical and Applied Mechanics SB RAS, Institutskaya str. 4/1, Novosibirsk, 630090, Russia

<sup>4</sup> Siberian State University of Water Transport, Schetinkina str. 33, Novosibirsk, 630099, Russia

E-mail: [kornienko\\_ee@mail.ru](mailto:kornienko_ee@mail.ru)

**Abstract.** This study considers the structural features of Ni-Cr-Si-B (Ni – base; 15.1 % Cr; 2 % Si; 2 % B; 0.4 % C) materials obtained by different methods. The self-fluxing coatings were deposited by plasma spraying on the tubes from low carbon steel. Bulk cylinder specimens of 20 mm diameter and 15 mm height were obtained by spark plasma sintering (SPS). The structure and phase composition of these materials were investigated by optical microscopy (OM), scanning electron microscopy (SEM), transmission electron microscopy (TEM) and X-ray diffractometry (XRD). The major phases of coatings and sintered materials are  $\gamma$ -Ni, Ni<sub>3</sub>B, CrB and Cr<sub>7</sub>C<sub>3</sub>. We demonstrate that the particle unmelted in the process of plasma spraying or SPS consist of  $\gamma$ -Ni-Ni<sub>3</sub>B eutectic and also CrB and Cr<sub>7</sub>C<sub>3</sub> inclusions. The prolonged exposure of powder to high temperatures as well as slow cooling rates by SPS provide for the growth of the structural components as compared to those of plasma coatings materials. High cooling rates at the plasma spraying by melted particles contribute to the formation of supersaturated solid solution of Cr, Si and Fe in  $\gamma$ -Ni. The structure of the melted particles in sintering material has gradient composition: the core constituted of Ni grains of 10  $\mu$ m with  $\gamma$ -Ni-Ni<sub>3</sub>B eutectic on the edges. The results of the experiment demonstrate that the sintering material has a smaller microhardness in comparison with plasma coatings (650 and 850 MPa, respectively), but at the same time the material has higher density (porosity less than 1 %) than plasma coatings (porosity about 2...3 %).

### 1. Introduction

The self-fluxing alloys of Ni-Cr-Si-B system possess high wear resistance [1-7] and corrosion resistance [2-5, 8-10] at room and higher temperatures and also high heat resistance [1, 3]. Due to these properties, machine details made of these materials are widely used in aerospace industry and aircraft construction [11], atomic [3, 12, 13], oil and chemical industry, and metallurgy [14].

There are many techniques of coatings deposition starting from the self-fluxing alloys, for example CVD and DVD [1], different kind of welding (laser cladding [15, 16], vacuum-arc deposition [17])



and thermal spraying (plasma spraying [6, 10, 18], flame spraying [1, 6, 7], high velocity oxy-fuel spraying [8, 9]). The technology of plasma spraying is widely used [6, 10, 18-23]. It allows to form coatings of any materials including composite coatings on surface of any complexity as well as restore the worn out machine parts surfaces. Unfortunately the disadvantages of plasma coatings are high porosity (up to 20 %) [7] and low adhesion [4, 5, 7, 18]. It may limit their use in corrosive mediums [4, 5, 8] and decrease their wear-resistance. The solution to of this problem is subsequent melting of self-fluxing coatings [2, 5, 7, 18].

SPS is perspective technique of high-pressure sintering. This method allows taking dense fine-grained material in short time [24]. In future this technique will be used for sintering of self-fluxing powders onto detail surface. The authors of study [25] demonstrate that dense coatings with high adhesion and high operation properties may form in that case. Nowadays significant amount of studies devoted to SPS were carried out [26-31], but there is no research into Ni-Cr-Si-B alloys sintering. Thus the questions about the structure and properties of these materials obtained by SPS require investigation.

In this study we consider the structural features of self-fluxing material of Ni-Cr-Si-B system obtained by plasma spraying and SPS.

## 2. Materials and methods

Coatings and bulk materials were formed from self-fluxing powder of Ni-Cr-Si-B system. Chemical composition of the powder: Ni – base; 15.1 % Cr; 2 % Si; 2 % B; 0.4 % C. The particle of self-fluxing powder had spherical form of 40...100  $\mu\text{m}$ .

Air-plasma spraying was carried out at the Institute of Theoretical and Applied Mechanics SB RAS with the help of plasmatron “PNK-50” with an annual injection of powder unit. The powder was sprayed on tubes from low carbon steel 20 (0.2 wt. % C). The inner diameter of tubes was 60 mm, the wall thickness was 3 mm. The regimes of plasma spraying were: current arc was 140 A, and voltage was 265 V. The blend of air and propane-butane was used as a carrier, focus and protective gas. The air was used as plasma gas. The distance of plasma spraying was 170 mm. Grit blasting of the substrate surface was performed before the spraying. Then the 75Ni15Al interlayer with thickness 10...15  $\mu\text{m}$  was deposited on the surface tubes to increase adhesion.

SPS was carried out at Tomsk Polytechnic University on the SPS10-4 apparatus. The regimes of sintering were: heating rate was 100  $^{\circ}\text{C}/\text{min.}$ , heating temperature was 1030  $^{\circ}\text{C}$ , sintering pressure was 65 MPa and the high-pressure treatment period at the sintering temperature was 5 min. We obtained the cylindrical specimens with diameter 20 mm and height 15 mm.

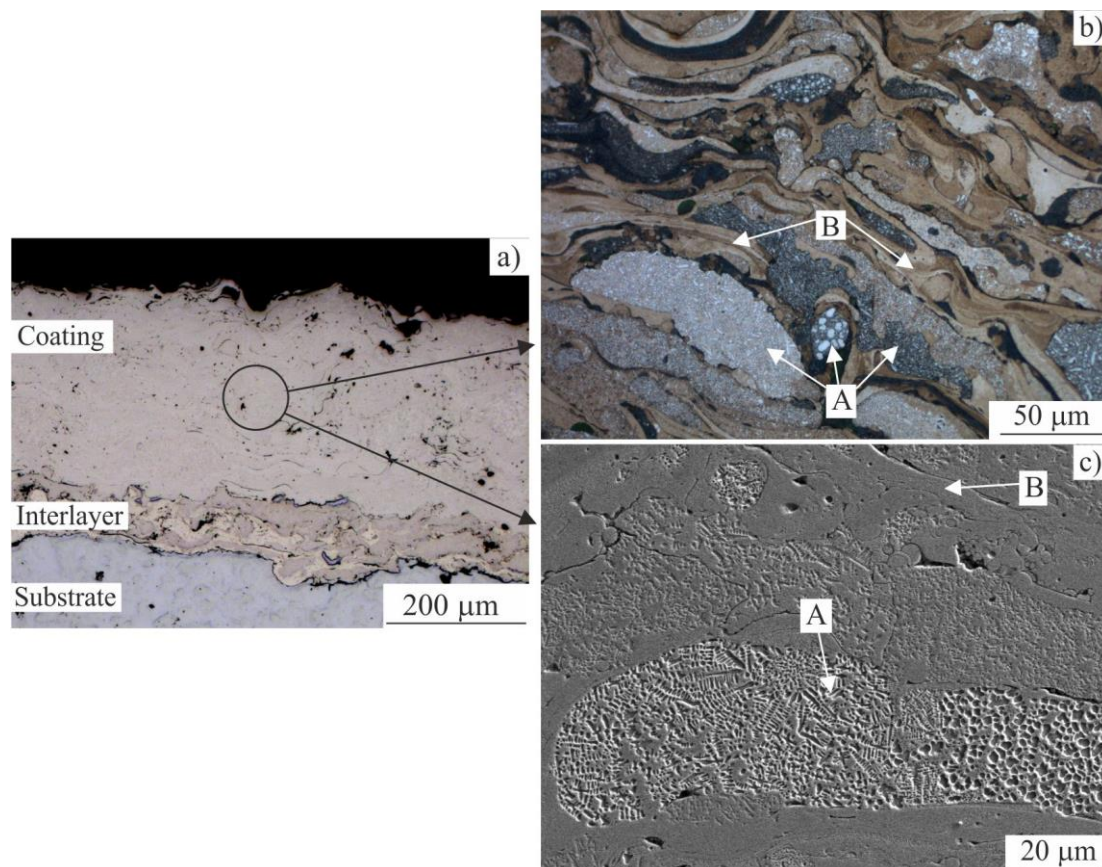
The microstructure of coatings and bulk material was identified by the optical microscope Carl Zeiss Axio Observer A1m and scanning electron microscope Carl Zeiss EVO50 XVP. The sample for analysis and microhardness measurement were cut by the cross-section and prepared by standard methods: mechanic grinding and polishing with colloidal  $\text{Al}_2\text{O}_3$ . To reveal eutectic the surface of the samples we etched it with the solution of 10 ml HCl, 0.1 ml  $\text{HNO}_3$ , and 10 g  $\text{FeCl}_3$ . Thin foils were cut from the middle of the coating for structural analysis by transmission electron microscope Tecnai G2 FEI. The XRD analysis was done using ARL X'TRA with  $\text{Cu K}_\alpha$  radiation. Microhardness was estimated by Wolpert Group 402MVD with pressure of 10 g.

## 3. Results and discussion

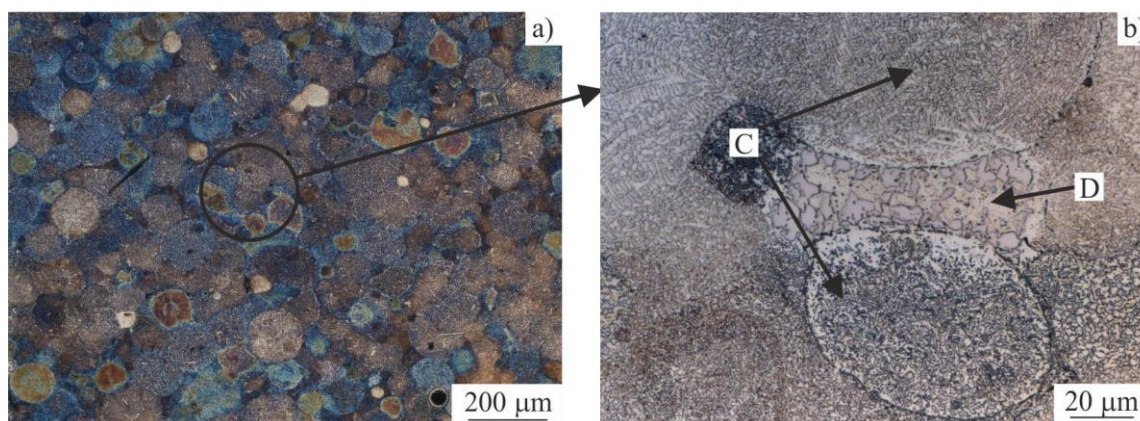
The structure of plasma coatings is presented in figure 1. We can observe that the material of coating contains slightly deformed and significantly deformed particles with the initial heterophase structure (A in Figures 1b, c). The major of powder particles melt in the process of plasma spraying. The supersaturated solid solution  $\gamma\text{-Ni}$  fixes on substrate or already consolidation material of coatings during crystallization process (B in Figure 1b, c) [32].

Figure 2 shows the material structure formed by SPS. The structural research allowed establishing that the most of particles do not change their form. It is clearly seen that the particles have contacts along the whole particle surface, providing for the material low porosity. The majority of particles

save their heterophase structure (C in Figure 2b). Small particles which are located in the joints of coarse particles are melted (D in Figure 2b).



**Figure 1.** The structure of coatings: a) before etching, b, c) after etching; a, b) OM, c) SEM.



**Figure 2.** The structure of sintering material.

According to the data obtained by X-ray diffraction (Figure 3), the major phases of self-fluxing coatings as well as sintering materials are  $\gamma$ -Ni,  $\text{Ni}_3\text{B}$ , CrB and  $\text{Cr}_7\text{C}_3$ . It is noteworthy that the initial powder has the same phase composition.

Figures 1c and 2b show that the structure of A and C type particles is identical and constitutes eutectic of  $\gamma$ -Ni dendrite and  $\text{Ni}_3\text{B}$  phase. The structure of A type particles is more disperse which can be explained by the short time exposure of powder particles to high temperature. In this case any

structural changes do not take place. The initial powder particles have the same disperse structure. The heating and cooling rates are less at SPS. The same conditions contribute to the transformation of material in a more stable state and lead to the changes that facilitate the increase of structural components.

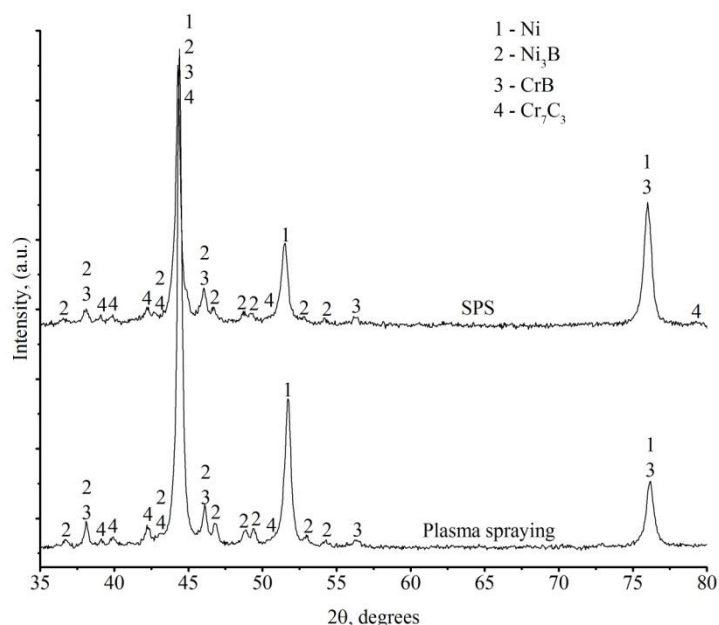


**Figure 3.** XRD spectra of the coating and sintering material.

According to the equilibrium diagram of Ni-C and Ni-B, C and B practically do not dissolve in Ni lattice (2.7 and 0.3 at. %, respectively) [33]. Chromium borides and carbides do not change their morphology in A type particles in comparison to the initial powder. Figure 4 obtained by SEM in regime backscattering electrons shows that the phases of these types are clearly seen. CrB is the dark-grey blocky particles, Cr<sub>7</sub>C<sub>3</sub> is light-grey with the flower shape. The size of these inclusions of plasma coatings is smaller, than the one of the sintering material (Figure 4b). It can be explained by the difference of the technology parameters.

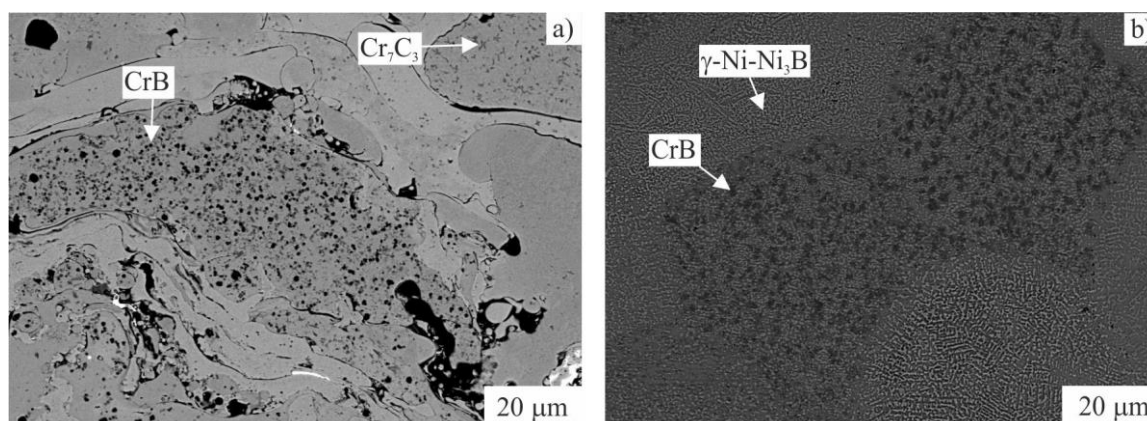


**Figure 4.** CrB and Cr<sub>7</sub>C<sub>3</sub> inclusions of coatings (a) and CrB inclusions of sintering material.

The structure of powder particles which were melted (B and D type) is also different. Significant supercooling degrees of B type particles do not allow segregating all alloying elements from  $\gamma$ -Ni lattice. As a result the coating particles of the same type constitute the supersaturated solid solution of

Cr, Si and Fe in  $\gamma$ -Ni. TEM revealed that the size of subgrain in the particles of this type does not exceed 100 nm (Figure 5). The structure of D type particles of sintering material is showed on figure 2b. Mostly, these particles represent coarse Ni grains with size up to 10  $\mu\text{m}$  in the particle core and  $\gamma$ -Ni-Ni<sub>3</sub>B eutectic about the particle edges.

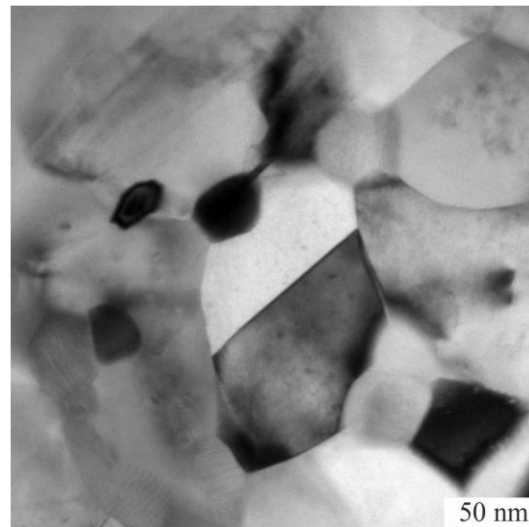


**Figure 5.** Bright-field image of the supersaturated solid solution of  $\gamma$ -Ni of coating.

It was revealed by microhardness measuring that the hardness of sintering material is less than coating (650 and 850 MPa, respectively). The study [34] by local microhardness measuring demonstrated that particles hardness changing depends on particles type. The slightly deformed particles have the smallest microhardness (600...700 HV). Figure 2a clearly shows that the sintering material is characterized by the presence of this type particles only. Besides long exposure of the material to high temperatures provides for the diffusion processes that further promote the decreases of the microhardness. The sintering material is denser (porosity less than 1 %) in comparison with plasma coatings (~2...3 %).

#### 4. Conclusions

X-ray analysis showed that the phase composition of coatings and sintering materials are the same. The major phases of coatings and sintering materials are  $\gamma$ -Ni, Ni<sub>3</sub>B, CrB and Cr<sub>7</sub>C<sub>3</sub>.

The OM and SEM revealed that the structure of plasma coatings and sintering materials are different. The unmelted particles in plasma jet or sintering constitute  $\gamma$ -Ni-Ni<sub>3</sub>B eutectic and CrB and Cr<sub>7</sub>C<sub>3</sub> inclusions. The prolonged exposure to high temperature of powder particles by sintering and low cooling rates provide the growth of structural components in comparison to material of plasma coatings. High cooling rates by plasma spraying of the melted particles contribute to formation of supersaturated solid solution of Cr, Si and Fe in  $\gamma$ -Ni. The structure of melted particles in sintering material has gradient composition: Ni grains with size up to 10  $\mu\text{m}$  are in the core of the particles and  $\gamma$ -Ni-Ni<sub>3</sub>B eutectic is about particles edges.

Microhardness measuring shows that sintering material has less hardness in comparison with plasma coatings (650 and 850 MPa, respectively).

Porosity measuring showed that sintering material is denser than coatings (porosity less than 1 % and about 2...3 %, respectively).

#### References

- [1] Chaliampalias D, Vourlias G, Pavlidou E, Skolianos S, Chrissafis K, Stergioudis G 2009 *Applied Surface Science* **255** 3605–3612

- [2] Hemmati I, Ocelik V and Hosson J Th M De 2013 *Physics Procedia* **41** 302-311
- [3] Sudha C, Shankar P, Rao R V S, Thirumurugesan R, Vijayalakshmi M and Raj B 2008 *Surface & Coatings Technology* **202** 2103–2112
- [4] Serresa N, Hlawka F, Costil S, Langlade C and Machi F 2011 *Applied Surface Science* **257** 5132–5137
- [5] Serres N, Hlawka F, Costil S, Langlade C and Machi F 2011 *Journal of Thermal Spray Technology* **20** 336-343
- [6] Gonzalez R, Garcia M A, Penuelas I, Cadenas M, Fernandez M del R, Battez A H and Felgueroso D 2007 *Wear* **263** 619–624
- [7] Zhang X C, Xu B S, Tu S T, Xuan F Z, Zhang Y K, Wang H D and Wu Y X 2009 *Fatigue & Fracture of Engineering Materials & Structures* **32** 84–96
- [8] Zhao W, Wang Y, Dong L, Wu K and Xue J 2005 *Surface & Coatings Technology* **190** 293–298
- [9] Lee C H and Min K O 2000 *Surface and Coatings Technology* **132** 49-57
- [10] Zeng Z, Kuroda S and Era H 2009 *Surface & Coatings Technology* **204** 69-77
- [11] Xuan H, Wang Q, Bai S, Liu Z, Sun H and Yan P 2014 *Surface & Coatings Technology* **244** 203–209
- [12] Guoqing C, Xuesong F, Yanhui W and Wenlong Z 2013 *Surface & Coatings Technology* **228** 276-282
- [13] Serres N, Hlawka F, Costil S, Langlade C and Machi F 2010 *Surface & Coatings Technology* **205** 1039–1046
- [14] Zhanga Z, Wangb Z and Liang B 2009 *Journal of materials processing technology* **209** 1368–1374
- [15] Pogrebnyak A D, Danilionok M M, Uglov V V, Erdybaeva N K, Kirik G V, Dub S N, Rusakov V S, Shpylenko A P, Zukovski P V and Tuleushev Y Zh 2009 *Vacuum* **83** 235–239
- [16] Li R, Li Z, Huang J, Zhanga P and Zhua Y 2011 *Applied Surface Science* **257** 3554–3557
- [17] Wulina S, Echigoya J, Beidi Z, Changsheng X and Kun C 2001 *Surface and Coatings Technology* **138** 291-295
- [18] Pogrebnyak A D, Danilionok M M, Uglov V V, Erdybaeva N K, Kirik G V, Dub S N, Rusakov V S, Shpylenko A P, Zukovski P V and Tuleushev Y Zh 2009 *Vacuum* **83** 235–239
- [19] Chesov Yu S, Zverev E A and Plokhov A V 2010 *Obrabotka metallov* **1** 14-8
- [20] Veselov S V et al 2010 *Obrabotka metallov* **4** 35-7
- [21] Lin C M 2012 *Journal of Thermal Spray Technology* **21** 873-881
- [22] Zhu H B, Li H and Li Z X 2013 *Surface & Coatings technology* **235** 620-627
- [23] Chesov Yu S et al 2014 *Obrabotka metallov* **65** 8-11
- [24] Tokita M 1993 *Journal of the Society of Powder Technology Japan* **30** 790–804
- [25] Raychenko A I 1987 *Osnovy protsessa spekaniya poroshkov propuskaniem elektricheskogo toka* (Moscow: Metallurgiya)
- [26] Kwon H, Jung S-A, Suh C-Y and Kim W 2016 *Ceramics International* **42** 8750–8753
- [27] Ding L, Xiang D P, Pan Y L, Zhang T M and Wu Z Y 2016 *Journal of Alloys and Compounds* **661** 136-140
- [28] Shongwe M B, Diouf S, Durowoju M O, Olubambi P A, Ramakokovhu M M and Obadeleb B A 2016 *International Journal of Refractory Metals and Hard Materials* **55** 16–23
- [29] Sadat T, Dirras G, Tingaud D, Ota M, Chauveau T, Faurie D, Vajpai S and Ameyama K 2016 *Materials & Design* **89** 1181–1190
- [30] Li Y, Katsui H, Goto T 2015 *Ceramics International* **41** 14258–14262
- [31] Shevtsova L I 2014 *Obrabotka metallov* **65** 21-27
- [32] Kornienko E E, Nikulina A A, Drobyaz E A, Plotnikova N V, Lapushkina E Yu and Kuz'min V I 2015 *Applied Mechanics and Materials* **788** 252-258.
- [33] Baker H 1998 *ASM Handbook Vol. 3: Phase Diagrams* (ASM International)
- [34] Kornienko E E, Smirnov A I, Kuz'min V I 2015 *Applied Mechanics and Materials* **698** 405-410